 https://doi.org/10.3311/PPci.20345

Periodica Polytechnica Civil Engineering, 66(4), pp. 1278–1293, 2022

Experimental Study on Size Effect and Fracture Properties of Polypropylene Fiber Reinforced Lightweight Aggregate Concrete

Alireza Hosseini Mehrab[1], M. Reza Esfahani[1*]

[1] Department of Civil Engineering, Ferdowsi University of Mashhad, Azadi Square, 9177948974 Mashhad, Iran
[*] Corresponding author, e-mail: esfahani@um.ac.ir

Received: 19 April 2022, Accepted: 28 August 2022, Published online: 12 September 2022

Abstract

In this experimental research, the effects of polypropylene fibers on size effect and fracture properties of lightweight aggregate concrete were studied. Two methods, including size effect method and work of fracture method, were used to investigate and analyze the size effect and fracture properties on different sizes of notched beams. The polypropylene fiber contents were 0.5%, 0.75%, and 1% by volume fraction. The obtained results revealed that increasing the polypropylene fibers in lightweight aggregate concrete relatively decreased the dependence of strength on the size effect parameter, while the addition of polypropylene fibers exhibited significant influence on decreasing the size dependency of ductility and fracture energy in lightweight aggregate concrete. Moreover, the increase of polypropylene fibers improved the total fracture energy (G_F), initial fracture energy (G_f), characteristic length (l_{ch}), length of fracture process zone (c_f), and critical stress intensity factor (K_{Ic}) of lightweight aggregate concrete in both size effect method and work of fracture method. This increase was more significant in work of fracture method because of considering the post-peak behavior. The size effect method was suitable and accurate for plain lightweight aggregate concrete. The G_F/G_f ratio increased from 2.88 in plain lightweight aggregate concrete to 12.26 in polypropylene fiber reinforced lightweight aggregate concrete.

Keywords

lightweight aggregate concrete, fracture energy, size effect, polypropylene fiber, characteristic length

1 Introduction

The application of lightweight aggregate concrete (LWAC) in structural elements such as high-rise buildings, large-span bridges, and offshore oil platforms has increased significantly due to the lower density, higher specific strength, durability, and insulation [1]. The low density of LWAC, which is the major benefit of LWAC, is achieved through incorporating porous lightweight aggregates. This property in LWAC resulted in economic benefits and reduced the risk of earthquake damage to the structures [2]. However, the LWAC exhibits greater brittleness than conventional concrete at comparable strength owing to the incorporation of porous lightweight aggregates [3]. This brittleness intensifies the expansion and development of cracks, earlier failure of the structure, and the effect of specimen size on strength, ductility, and fracture behavior in LWAC compared to conventional concrete and restricts the further application of LWAC in the construction industry [4].

The use of fibers in LWAC has been suggested by many researchers in order to decrease the expansion of cracks and improve ductility [5, 6]. In general, fibers can be classified into metallic, synthetic, and natural. Synthetic fibers such as polyvinyl, polyolefin, and polypropylene have attracted significant attention in LWAC due to their high performance [7, 8]. Polypropylene fiber has been recognized as the most widely used synthetic fiber in LWAC due to its high ductility, chemical durability, low price, and low specific gravity [9]. The polypropylene fibers not only decrease the weight of LWAC but also increase the ductility and energy absorption of LWAC. The most important reason for this mechanism is attributed to the bridging of polypropylene fibers in impeding the expansion of cracks [10]. The main effect of polypropylene fibers in LWAC begins when the cracks initiate and propagate, in which the polypropylene fibers prevent the further growth of cracks and increase the post-peak behavior of LWAC [11].

Cite this article as: Hosseini Mehrab, A., Esfahani, M. R. "Experimental Study on Size Effect and Fracture Properties of Polypropylene Fiber Reinforced Lightweight Aggregate Concrete", Periodica Polytechnica Civil Engineering, 66(4), pp. 1278–1293, 2022. https://doi.org/10.3311/PPci.20345

In recent years, fracture mechanics science, which considers the crack initiation and propagation in concrete and the effect of fibers on the toughness of concrete, has been considered by many researchers to study the behavior of various fiber reinforced concretes [12]. One of the main characteristics of fracture behavior of concrete is the fracture energy, which indicates the energy absorption and crack resistance of materials [13]. Different methods, which the most important ones include work of fracture method (WFM) based on fictitious crack model by RILEM TC-50 FMC [14] and size effect method (SEM) based on elastic crack model by RILEM TC-89 [15], were used to analyze the fracture properties of fiber reinforced concrete [16, 17]. Most of studies on the fracture properties of fiber reinforced lightweight aggregate concrete (FRLWAC) were conducted using WFM [11, 18]. Rasheed et al. [19] investigated the effects of polyolefin fibers on the fracture properties of LWAC. They observed an increase in the total fracture energy obtained from WFM due to the addition of polyolefin fibers. Li et al. [11] demonstrated that the addition of 0.3% and 0.6% volume fraction of polypropylene fibers enhanced the total fracture energy obtained from WFM at ambient temperature in LWAC. However, these studies did not investigate the size dependency of total fracture energy derived from WFM in FRLWAC. The major reason for using fracture mechanics science is the size effect parameter, which plays an important role in the strength, ductility, and fracture properties of different types of concrete [20]. Many researchers studied the size effect on the mechanical properties and fracture behavior of various plain concretes, particularly the LWAC due to its brittleness [4, 21]. However, only a number of studies investigated the size effect on the fracture response of fiber reinforced concrete [22, 23]. Ghasemi et al. [22] researched the effect of steel fibers on self-compacting concrete using SEM and pointed out that the steel fibers relatively decreased the effect of specimen size on the fracture behavior. However, they did not comprehensively study this effect on strength, ductility, and fracture behavior of notched beams. Nguyen et al. [24] studied the influence of size effect parameter on the flexural behavior of ultra-high performance hybrid fiber reinforced concrete and resulted in that the flexural behavior of this concrete was more sensitive to the size of specimens when low volume contents of fibers were employed. However, they only investigated the size effect on mechanical properties, and the size effect on fracture criteria was neglected.

Although the fracture and mechanical properties of FRLWAC have been studied by some researchers and it has drawn the attention of engineers who wish to utilize FRLWAC in structural aspects, the fracture and mechanical properties of FRLWAC used in various sizes might be different owing to the size effect parameter. According to the previous studies, no evident study has investigated the size effect on fracture response and mechanical properties of FRLWAC. Moreover, it sounds that the fracture properties of FRLWAC require more reviews, especially by other fracture mechanics methods such as SEM. This situation was the motivation for this experimental study, in which notched beams with different sizes were investigated using SEM and WFM according to RILEM recommendations [14, 15], focusing on fracture properties and size effect on fracture response, strength, and ductility. The polypropylene fiber type with different volume contents of 0.5%, 0.75%, and 1% was incorporated in LWAC. The main aims of this experimental research are to study (1) the influence of size effect parameter on the strength, ductility, and fracture properties of polypropylene fiber reinforced lightweight aggregate concrete (PFLWAC), and (2) the influence of polypropylene fibers on size effect and fracture properties in LWAC employing both SEM and WFM. Moreover, the relationships between the specimen size, the dosage of polypropylene fibers, and fracture parameters were determined by utilizing a commercial program called Design-Expert [25] based on the response surface method.

2 Theories of size effect and fracture parameters

2.1 Size effect method (SEM)

The size effect in structural designs is the most important reason for using fracture mechanics analysis in concrete structures. The most important influence of the size effect parameter is the decrease in the strength and ductility of structures due to the increase in its size. Three various approaches, including statistical, deterministic, and fractals, were presented to explain the size effect on the behavior of concrete [23]. Among these approaches, the deterministic approach, which is Bažant's theory based on fracture mechanics, was used in most studies [20]. Bažant presented size effect theory from a deterministic approach by employing fracture mechanics for quasi-brittle materials such as concrete [26, 27]. Bažant [27] explained this theory by presenting nominal strength (σ_N) as follows:

$$\sigma_N = Bf_t\left(1+\frac{D}{D_0}\right)^{-1/2}, \quad (1)$$

where f_t is the size-independent tensile strength of materials, D is the size of specimen, D_0 is a parameter based on structural geometry, and B is a dimensionless constant parameter indicating the solution according to plastic limit analysis based on the strength method. Both B and D_0 are based on the type of materials and geometry of specimens. The effect of size on the strength of materials for a series of geometrically similar structures with different sizes is shown in Fig. 1. The horizontal dashed line in Fig. 1 shows the strength criterion, which is a constant regardless of structural size and may only be used for relatively small size structures. The inclined dashed line with a slope of –1/2 in Fig. 1 illustrates the linear elastic fracture mechanics (LEFM), which may be used for relatively large size structures. By employing fracture mechanics approaches, a nonlinear curve (nonlinear fracture mechanics (NLFM)) between the size of structures and strength can be established, which for small size structures is close to the strength criterionand for large size structures is close to the LEFM [20].

Apart from the size effect on strength, there is another size effect, which is on the ductility of the structures, and it can be characterized by the deformation at which the structure fails under a given type of loading [28]. The primary influence of this size effect is on the descending branch or the post-peak response of the load-deflection curve. Fig. 2 illustrates the stress-relative deflection curves of geometrically similar structures with different sizes. In this curve, the relative deflection can be explained by the δ/D ratio, in which the δ is the deflection and D is the characteristic dimension of the structures [20]. It can be seen in Fig. 2 that the post-peak response for small structures descends slowly. In comparison, it descends steeper as the size of specimens increases. It has even shown a snapback for sufficiently large structures. Since the large structures have more considerable strain energy to propagate the failure zone and overcome the fracture process zone compared to small structures, the large structures show smaller ductility than the small structures [20].

Later, Bažant and Kazemi [29] simulated the size effect and fracture of quasi-brittle materials such as concrete by an effective-elastic crack model. They proposed the SEM for a series of geometrically similar specimens with different sizes under three-point bending tests. This method only requires the maximum applied load (P_{max}) of each specimen. The fracture parameters resulting from this

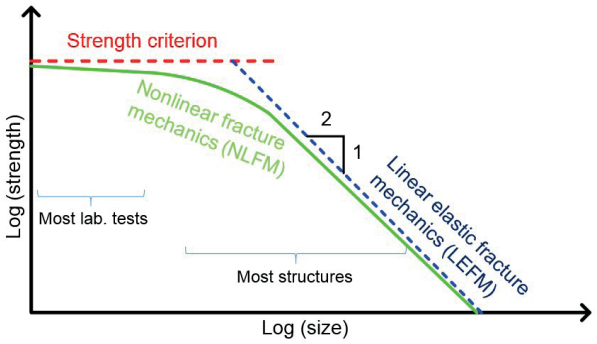

Fig. 1 Size effect on the strength of materials

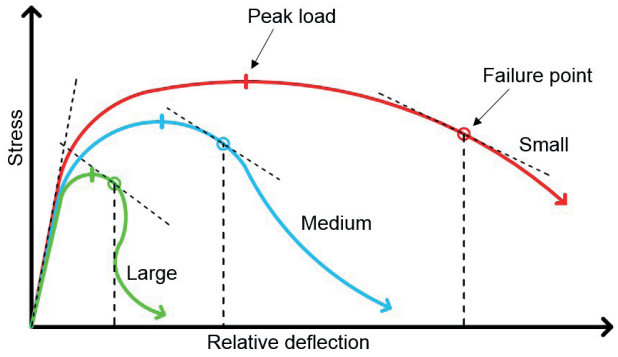

Fig. 2 Size effect on the ductility of structures

method are independent of the specimen size. The SEM was studied according to RILEM TC-89 [15]. In addition, the (P_{max}) was calculated as the corrected maximum load (P_0) for each specimen.

The nominal strength (σ_N) for geometrically similar notched beams is determined using Eq. (2) as follows:

$$\sigma_N = \frac{Bf_t}{\sqrt{1+\beta}}, \beta = \frac{d}{d_0}, \quad (2)$$

where β is the brittleness number [20]. Once $\beta < 0.1$, the concrete behavior is ductile, and it is similar to that of the strength criterion. The concrete behavior is nonlinear when $0.1 \le \beta \le 10$, and when $\beta > 10$, the behavior of concrete is linear and close to the LEFM. As mentioned earlier, the two parameters of B and d_0 are experimental coefficients depending on the type of materials and geometry of specimens, which could be estimated as follows using regression analysis:

$$Y = AX + C,\ X = d,\ Y = \left(\frac{1}{\sigma_N}\right)^2,\ d_0 = \frac{C}{A},\ B = \frac{1}{\sqrt{C}}, \quad (3)$$

in which A shows the slope and C is the Y-intercept of the regression line. Bažant and Kazemi [29] showed that the initial fracture energy (G_f), the length of fracture process zone (c_f), and the critical stress intensity factor (K_{Ic}) could be calculated as follows:

$$G_f = \frac{g(\alpha_0)}{E \times A}, \tag{4}$$

$$c_f = \frac{g(\alpha_0)}{g'(\alpha_0)}\left(\frac{C}{A}\right), \tag{5}$$

$$K_{Ic} = \sqrt{EG_f}, \tag{6}$$

where E is the modulus of elasticity, $g(\alpha_0)$ is the dimensionless geometric factor of the energy dissipation rate, which should be calculated by $\alpha_0 = a_0/d$ according to RILEM TC-89 [15], and $g'(\alpha_0)$ is the value of the first derivative of $g(\alpha_0)$.

2.2 Work of fracture method (WFM)

One of the simplest and the most common methods to calculate fracture parameters of concrete is the WFM. This method has been proposed based on the fictitious crack model of Hillerborg et al. [30]. In this method, three-point bend notched beams (Fig. 3) were used to calculate the total fracture energy (G_F) and the characteristic length of concrete (l_{ch}) [13]. The G_F is the energy required to create a crack at the unit surface. By determining the load-midspan displacement curve (Fig. 4) for the three-point bend notched beam and then dividing the work by the initial ligament area ($b(d - a_0)$), the fracture energy G_F could be estimated as follows:

$$G_F = \frac{w_t}{b(d-a_0)} = \frac{w_0 + w_1 + w_2}{b(d-a_0)} = \frac{w_0 + 2P_w\delta_0}{b(d-a_0)}, \tag{7}$$

where w_t represents the total area under the load-midspan displacement curve (P–δ) (Fig. 4), w_0 shows the area below the P_a–δ curve, and is equal to $P_w \times \delta_0$. An equivalent force P_w represents the influence of concrete beam self-weight, and δ_0 is the displacement corresponding to $P_a = 0$ [13, 30]. w_2 is considered approximately equal to w_1 [31, 32].

The characteristic length of concrete (l_{ch}) is a pure material property of concrete and is proportional to the length of the fracture process zone based on the fictitious crack model. Hillerborg [33] also introduced the l_{ch} to express the concrete ductility. The l_{ch} could be calculated as follows:

$$l_{ch} = \frac{E \times G_F}{f_t^2}, \tag{8}$$

where E is the modulus of elasticity and f_t represents the tensile strength of concrete.

The fracture energy obtained from this method is also dependent on the shape and the size of specimens [4, 34]. This size dependency may be due to the existence of fracture process zone in front of the extending crack and the unwanted energy absorption outside the fracture process zone [29]. This unwanted energy absorption increases as the size of structures increases. Some studies indicated that the main reasons for the unwanted energy absorption are experimental errors such as testing equipment, friction of supports, bulk energy dissipation, weight of specimens, and cutting the tail of load-deflection curve [35–38]. To decrease the effects of the mentioned errors in these beams, the following proceedings were proposed: calibration of testing equipment, utilization of rolling supports to prevent the friction and crushing of supports, considering the weight of samples and attached devices in the measurement, and the calculation of the area below the load-midspan deflection curve measured up to the deflection at zero loading [36–38]. Although the fracture energy may be more or less size-independent by considering these errors in calculating fracture energy, the fracture energy may still be size-dependent [13].

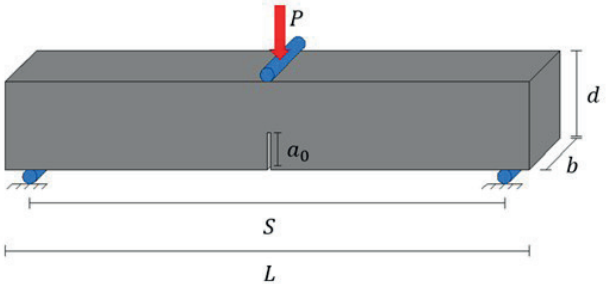

Fig. 3 Three-point bend notched beam

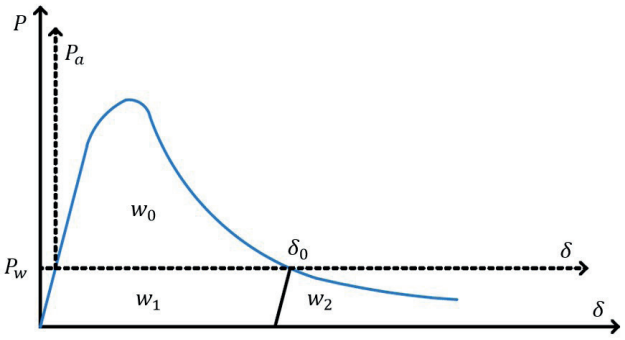

Fig. 4 Load-midspan displacement curve of notched beam

3 Experimental work

3.1 Materials

The cement used in this research was Portland cement type II. The industrial expanded shale lightweight aggregate with the particle size of 4.75-19 mm was used as coarse aggregates. The quality characteristics of lightweight aggregates were tested based on CS GB/T17431.2 [39].

The natural river sand with a fineness modulus of 2.79 and a nominal maximum size of 4.75 mm was utilized. The silica fume was employed by 10% of the weight of cement. Table 1 represents the chemical and physical properties of cement, silica fume, and lightweight aggregate. The properties of polypropylene fibers are shown in Table 2. A carboxylate-based superplasticizer prepared with 1.08 g/cm^3 specific gravity was also employed to reduce the water content and keep the workability based on slump test (ASTM C143-05 [40]) in the range of 40–70 mm in mixtures.

3.2 Mix design and preparation

Four mix designs, including plain lightweight aggregate concrete (LWAC) and lightweight aggregate concretes with volumetric content of polypropylene fibers (V_{pf}) of 0.5%, 0.75%, and 1% (PFLWAC-0.5, PFLWAC-0.75, and PFLWAC-1, respectively) were prepared. Table 3 depicts the concrete mixtures.

For the production of mixtures, the fine and coarse aggregates were mixed for 5 minutes. The polypropylene fibers were added to it during the mixing of aggregates. This mixing method prevents the polypropylene fibers from balling in the concrete as much as possible [5]. Afterward, the cement and silica fume were added to the mixture and allowed to mix for about 2 minutes. Water and superplasticizer were then gradually added to the combination over 2 minutes. Finally, the mixing continued for 2 minutes. After casting concrete in the molds and compacting by vibration, the samples were demolded following 24

Table 1 Chemical and physical properties of materials

Chemical compounds (%)	Materials		
	Cement	Silica fume	Lightweight aggregate
SiO_2	21.0	93.6	58.48
Al_2O_3	4.6	1.3	16.57
Fe_2O_3	3.9	0.3	6.65
CaO	62.5	0.49	2.33
MgO	2.9	0.97	2.3
SO_3	2.0	0.1	0.4
Na_2O	0.5	0.31	1.4
K_2O	0.45	1.01	2.91
L . O . I	1.4	….	7.37
SiC	….	0.5	….
C	….	0.3	….
P_2O_5	….	0.16	0.16
TiO_2	….	….	0.77
Physical properties			
Specific gravity (g/cm^3)	3.15	2.21	-
Particle density (g/cm^3)	-	-	1.06
Cement compressive strength, 28 days (MPa)	49.5	-	-
Autoclave expansion (%)	0.08	-	-
Fineness, Blaine test (cm^2/g)	3200	-	-
1 h water absorption (%)	-	-	11.6
24 h water absorption (%)	-	-	13.1
Cylinder compressive strength (MPa)*	-	-	10.8

* CS GB/T17431 [39]

Table 2 Properties of polypropylene fibers

Specific gravity (g/cm^3)	Elastic Modulus (GPa)	Tensile strength (MPa)	Length (mm)	Diameter (mm)	Melting point (°C)
0.91	6.0	400	12	0.035	160-170

Table 3 Mix proportions of concrete mixtures

Materials	Mixtures			
	LWAC	PFLWAC-0.5	PFLWAC-0.75	PFLWAC-1
Cement (kg/m^3)	450	450	450	450
Silica fume (kg/m^3)	50	50	50	50
Lightweight aggregates (kg/m^3)	350	350	350	350
Sand (kg/m^3)	765	765	765	765
Superplasticizer (kg/m^3)	1.8	4	5	6.5
Water (kg/m^3)	188.2	188.2	188.2	188.2
Volume contents of polypropylene fibers, V_{pf} (%)	0	0.5	0.75	1
Unit weight (kg/m^3)	1805	1807	1808	1810
Slump (mm)*	70	50	48	45

* ASTM C143 [40]

hours. To prevent lightweight aggregate water absorption, the lightweight aggregates were pre-soaked in water for 1 hour prior to mixing the concrete [41]. All the specimens were cured for 28 days.

3.3 Test procedures

Nine geometrically similar notched beams under the three-point bending test were prepared according to RILEM TC-89 [15] for each mixture to investigate the size effect on strength and determine the fracture parameters through the SEM. The load-midspan deflection curves of these beams were also measured by a linear variable differential transformer (LVDT) with a range up to 5 mm was used for plain and polypropylene fiber reinforced LWAC to investigate the size effect on ductility and fracture energy (Fig. 5). The width (b) was constant and equal to 70 mm, and three sizes were considered for depth of beams (d), 70, 140, and 280 mm. For each depth size (d), three similar notched beams were prepared. In these beams, the width of the notch was taken 3 mm. The determination of the other dimensions in these beams is illustrated in Fig. 6. Three notched beams with dimensions of 350 × 100 × 100 mm (length × width × depth) under the three-point bending test were prepared for each mixture according to RILEM TC-50 FMC [14] in order to study the fracture properties of WFM. In these beams, the notch depth (a_0) was 33% of the beam depth (d), and the length of span (S) was 300 mm. Moreover, the width of the notch was also taken 3 mm. Following 28 days of curing, all the notched beams were loaded based on RILEM recommendations [14, 15]. Constant displacement rates were imposed such that the maximum load happened at about 1 min and 5 min in WFM and SEM notched beams, respectively. To determine the mechanical characteristics for each mixture, the compressive strength of concrete was determined using 150 × 150 × 150 mm cubic specimens according to BS EN 12390 [42]. Cylindrical specimens with dimensions of 100 × 200 mm were made to determine the splitting tensile strength based on ASTM C496-11 [43]. The modulus of elasticity test was performed on 150 × 300 mm cylindrical specimens based on ASTM C469-04 [44].

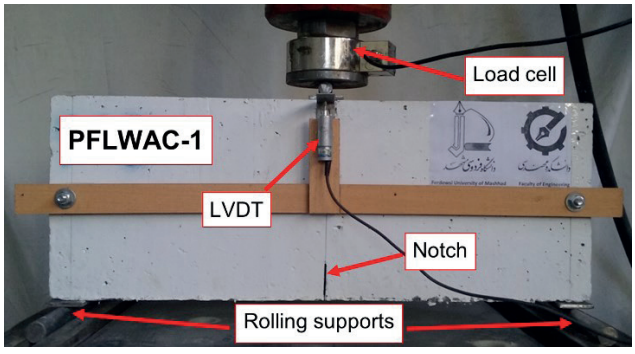

Fig. 5 The test setup

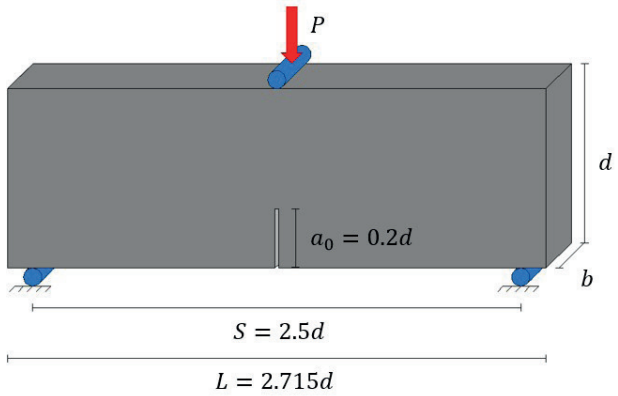

Fig. 6 Dimensions in SEM beams

4 Results and discussion

4.1 Fracture parameters of SEM

As mentioned earlier, only the peak load obtained from the geometrically similar notched beams under the three-point bending test is required to calculate the main fracture parameters such as initial fracture energy, length of fracture process zone, and stress intensity factor in SEM. The corrected maximum loads (P_0) of all the mix designs are exhibited in Table 4. Table 5 demonstrates the results of SEM fracture parameters. Fig. 7 illustrates the linear regression results of LWAC, in which the line slope of $A = 0.0106$ and y-intercept of $C = 1.0537$ was obtained with the correlation coefficient of $R^2 = 0.9536$. According to RILEM TC-89 [15], the variation coefficient of slope (ω_A),

Table 4 Maximum corrected loads in SEM

Mixtures	Size	d (mm)	Corrected maximum load (N)		
			Beam 1	Beam 2	Beam 3
LWAC	Small	70	3677.9	3858.1	3588
	Medium	140	6521.6	5692.2	6071.9
	Large	280	9996.7	9858.8	9547.5
PFLWAC-0.5	Small	70	4198.1	3883.2	4567.9
	Medium	140	7061.4	6742.8	7980
	Large	280	11131.2	11396.6	11832.5
PFLWAC-0.75	Small	70	4718.2	4078	4787.7
	Medium	140	8242.9	7352.2	7950.9
	Large	280	12621.5	12058.6	12363.7
PFLWAC-1	Small	70	3827.7	3958	4457.9
	Medium	140	7100.9	7762.3	6681.5
	Large	280	12113.5	11239	10906

Table 5 The fracture parameters of SEM

Mixtures	f_c (MPa)	E (GPa)	f_t (MPa)	a_0/d	$g(\alpha_0)$	G_f (N/m)	c_f (mm)	B_{ft} (MPa)	d_0 (mm)	K_{IC} (MPa$\sqrt{\text{mm}}$)	ω_A	ω_C	m
LWAC	40.2	18.5	2.2	0.2	7.3	36.9	18.3	1	95.9	26.1	0.07	0.13	0.12
PFLWAC-0.5	40.7	18.4	2.8	0.2	7.3	52.9	21	1.1	110.1	31.2	0.11	0.2	0.19
PFLWAC-0.75	41.1	18.2	3.3	0.2	7.3	62.6	21.3	1.2	111.5	33.8	0.1	0.17	0.17
PFLWAC-1	40.4	18	2.9	0.2	7.3	56.2	24.4	1	127.8	31.8	0.14	0.2	0.22

the variation coefficient of intercept (ω_C), and the relative width of scattering bond (m) should not exceed 0.1, 0.2, and 0.2, respectively. As shown in Table 5, some values of the three parameters of ω_A, ω_C, and m, were slightly greater than 0.1, 0.2, and 0.2, respectively. One of the main reasons could be using large amounts of fibers in concrete, which caused dispersion in the values of peak loads and consequently scattered these three parameters [16, 17].

One of the main characteristics of fracture behavior of concrete is the fracture energy, which indicates the energy absorption and crack resistance of materials [13]. The addition of 0.5%, 0.75%, and 1% volume content of polypropylene fibers increased the initial fracture energy (G_f) of LWAC significantly. The reason for the increase in initial fracture energy was that the polypropylene fibers delayed the initiation of cracks, limited the expansion of cracks, and consequently increased the load-bearing capacity of notched beams. Using Design-Expert [25] and analyzing the experimental results, a relationship has been suggested for G_f in the current research that depends on the volume content of polypropylene fibers, V_{pf} (%):

$$G_f = 36.58 + 55.54V_{pf} - 34.51{V_{pf}}^2 \left(R^2 = 0.947\right). \quad (9)$$

The fracture process zone (c_f) is one of the important features presented in the SEM, which indicates the ductility of materials. As shown in Table 5, the value of c_f enhanced as the polypropylene fiber volume contents increased in LWAC. Thereby, the LWAC becomes more ductile. Another point is that the G_f had the highest value at 0.75% volume content of polypropylene fibers, while a decrease in the amount of G_f could be seen at 1% volume content of polypropylene fibers. On the other hand, the value of c_f reached its highest amount at 1% volume content of polypropylene fibers. This result indicates that although using larger amounts of polypropylene fibers, more than 0.75% in LWAC decreased the load-bearing capacity, it had its positive role in increasing ductility. The same trend was reported in the research performed by Ghasemi et al. [22] for incorporating steel fibers in self-compacting concrete.

Another important parameter in SEM is the stress intensity factor (K_{IC}), which is also called fracture toughness. Table 5 shows that the K_{IC} of LWAC increased as the polypropylene fibers were added to the mixtures, which indicated the greater resistance of PFLWAC against unstable crack initiation and propagation. The reason for this increase in the amounts of the K_{IC} was that the polypropylene fibers delayed the crack initiation and propagation, thereby increasing the load-bearing capacity of the sample. Thus, the LWAC undergo more ductile fracture. By analyzing the results of K_{IC}, the relationship based on the V_{pf} (%) is as follows:

$$K_{Ic} = 25.96 + 17.18V_{pf} - 10.93{V_{pf}}^2 \left(R^2 = 0.94\right). \quad (10)$$

The brittleness number (β) in SEM is one of the fracture characteristics of concrete, which was presented to determine the fracture mode [15]. Fig. 8 represents the brittleness number of each beam. In all the mix designs, the brittleness number of small (d = 70 mm), medium (d = 140 mm),

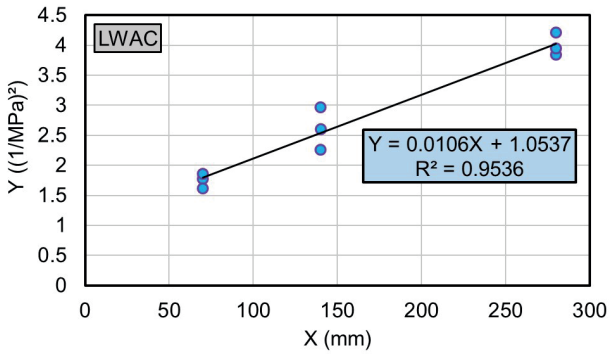

Fig. 7 Linear regression of LWAC

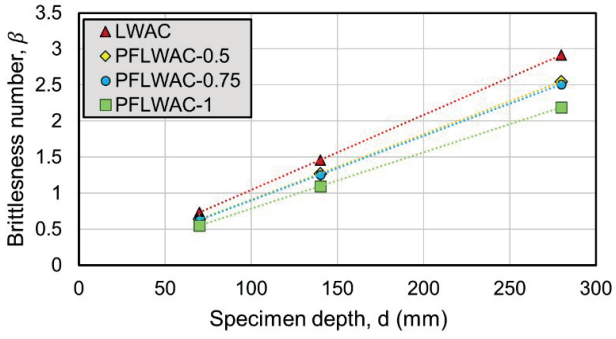

Fig. 8 Brittleness number for each mixture

and large (d = 280 mm) beams ranged between 0.1 and 10, which indicates that all the mix designs had nonlinear behavior [29]. Moreover, the brittleness number increased by increasing the specimen size compared to the effective length of fracture process zone of concrete. This increase in the value of brittleness number approached the behavior of LWAC to LEFM.

On the other hand, the incorporation of polypropylene fibers in LWAC decreased the brittleness number in Fig. 8. The highest decrease in the amount of brittleness number of LWAC was due to the addition of 1% volume content of polypropylene fibers, which decreased the brittleness number of specimens by 24.9%. Therefore, the polypropylene fibers could decrease the brittleness and enhance the ductility of LWAC.

Fig. 9 demonstrates Bažant's size effect curve fitted by the experimental data from four mix designs. According to Bažant's size effect curve, the more ductile the concrete is, the closer its behavior is to the strength criterion, and the more brittle the concrete is, the closer its behavior is to the LEFM [20]. Fig. 9 also demonstrates that the small size specimens were closer to the strength criterion. However, the behavior of large specimens approached the LEFM. Thus, the behavior of small specimens was ductile, and the behavior of large specimens was brittle in LWAC. Moreover, it can be concluded that the LEFM is more logical to design large specimens, while the strength criterion is more logical for modeling small specimens. On the other hand, the incorporation of polypropylene fibers led to approaching the behavior of specimens to the strength criterion. This result shows that the polypropylene fibers effectively improved the ductile behavior of LWAC.

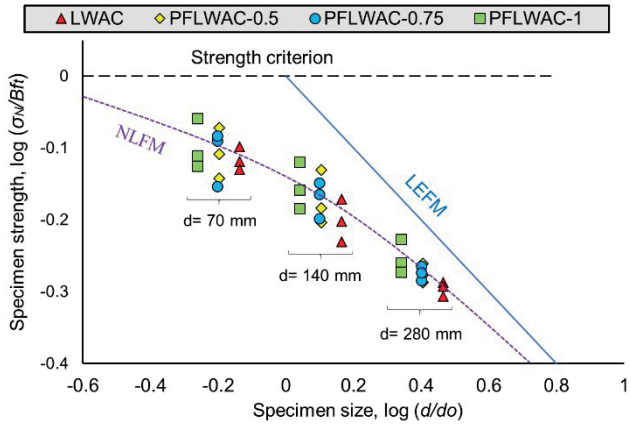

Fig. 9 Size effect plot constructed for all mix designs

4.2 Fracture parameters of WFM

In WFM, the total fracture energy (G_F) indicates the amount of energy consumed to create cracks per unit area [18, 33]. The G_F can be determined by measuring the area under the load-midspan deflection curve of three-point bend notched beams (Fig. 10). In this research, this area was calculated up to the deflection of 5 mm in 350 × 100 × 100 mm (length × width × depth) notched beams. Fig. 11 depicts the results of fracture parameters for each mixture. It can be seen in Fig. 11 that the incorporation of polypropylene fibers increased the G_F in LWAC. The main reason for this increase was that the polypropylene fibers delayed the expansion of cracks and increased the load-bearing capacity and post-peak behavior of notched beams. The relationship for predicting G_F is as follows:

$$G_F = 97.5 + 1639.2V_{pf} - 979.5V_{pf}^2 \left(R^2 = 0.945\right). \quad (11)$$

In addition, it can be seen in Fig. 10 that increase of polypropylene fibers led to higher deflection and smaller slope in the post-peak response of the curves, which exhibited more ductile behavior in LWAC. Another important

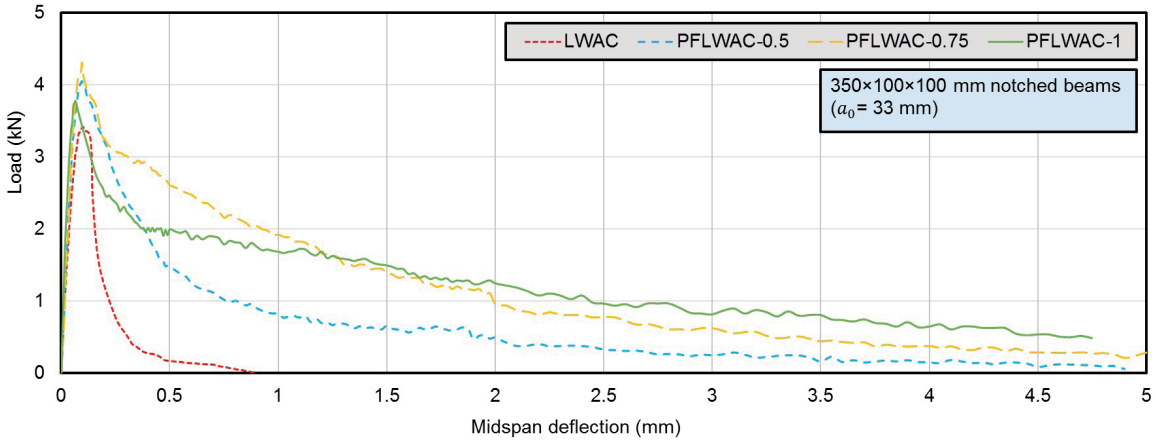

Fig. 10 Load-midspan deflection curves of 350 × 100 × 100 mm notched beams

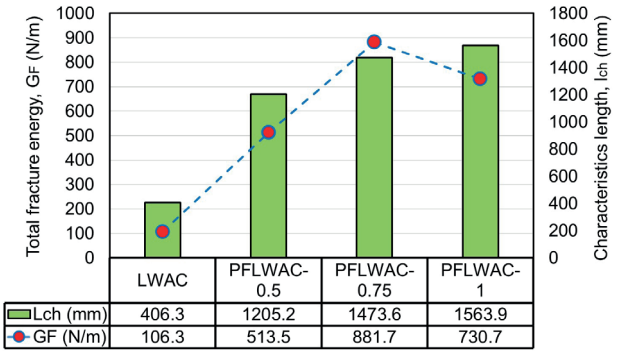

Fig. 11 The fracture parameters of WFM in 350 × 100 × 100 mm beams

parameter in WFM is the characteristic length (l_{ch}), which expresses the ductility of materials and is the opposite of brittleness [18]. According to Fig. 11, the l_{ch} enhanced as the polypropylene fiber volume contents increased by 1% in LWAC. As a result, the increase in l_{ch} on account of the increase of polypropylene fibers in LWAC exhibited lower brittleness and more ductile behavior. Such results following the addition of polypropylene fibers in LWAC have also been reported in previous research [11, 45]. The relationship between the V_{pf} (%) and the l_{ch} (mm) is expressed as follows:

$$l_{ch} = 404.4 + 2095.7V_{pf} - 928.8{V_{pf}}^2 \left(R^2 = 0.99\right). \quad (12)$$

According to the fracture parameters in Table 5 and Fig. 11, the increase in G_F obtained from WFM owing to the addition of 0.5%, 0.75%, and 1% volume fraction of polypropylene fibers was significantly greater than the increase in G_F obtained from SEM. In SEM, the maximum load is sufficient to determine the G_F, whereas, in WFM, the total area below the load-midspan deflection curve is needed to determine the G_F. As seen in Fig. 10, the polypropylene fibers increased the area under the load-midspan deflection curve greater than the load-bearing capacity in PFLWACs. Therefore, the results of G_F derived from WFM were much greater than the results of G_F derived from SEM in LWAC and PFLWACs.

4.3 Size effect on the material strength

One of the effects of specimen size is on the strength of materials. Bažant demonstrated this effect by introducing the nominal strength (σ_N) according to the size effect law [20]. The nominal strength results obtained from Bažant's size effect law for all the mix designs are illustrated in Table 6. Table 6 implies that as the size of notched beams increased from small to large, the nominal strength in each mixture decreased, respectively. This decrease in the amount of nominal strength indicates the size dependency of strength and shows that the strength of larger notched beams sustained lower loads and had higher probability of failure than did the smaller notched beams. The nominal strength in LWAC decreased by 34.2% as the beam size increased from small to large. However, the increase in the volume fraction of polypropylene fibers in LWAC reduced this decrease in the amount of nominal strength as the beam size increased. This mechanism demonstrates that the polypropylene fibers in LWAC relatively reduced the dependence of the specimen strength on the size effect.

The important point is that the polypropylene fibers reduced the decrease of nominal strength as the beam size increased from small to medium, while the polypropylene fibers did not reduce the decrease of nominal strength as the beam size increased from medium to large. When the

Table 6 The nominal strength (of each mix design

Mixtures	f_c (MPa)	f_t (MPa)	E (GPa)	βf_t	Size	d (mm)	d/d_0	σ_{N1} (MPa)	σ_{N2} (MPa)	σ_{N3} (MPa)	$\sigma_{N\,ave}$ (MPa)	C.V. (%)
					Small	70	0.7	0.75	0.79	0.73	0.76	0.08
LWAC	40.2	2.2	18.5	1	Medium	140	1.5	0.66	0.58	0.64	0.63	0.18
					Large	280	2.9	0.51	0.5	0.49	0.5	0.01
					Small	70	0.6	0.86	0.79	0.93	0.86	0.38
PFLWAC-0.5	40.7	2.8	18.4	1.1	Medium	140	1.3	0.72	0.69	0.81	0.74	0.35
					Large	280	2.5	0.57	0.58	0.6	0.58	0.03
					Small	70	0.6	0.96	0.83	0.98	0.92	0.48
PFLWAC-0.75	41.1	3.3	18.2	1.2	Medium	140	1.3	0.84	0.75	0.81	0.8	0.18
					Large	280	2.5	0.64	0.62	0.63	0.63	0.01
					Small	70	0.6	0.78	0.81	0.91	0.83	0.37
PFLWAC-1	40.4	2.9	18	1	Medium	140	1.1	0.72	0.79	0.68	0.73	0.28
					Large	280	2.2	0.62	0.57	0.56	0.58	0.12

beam size increased from small to medium, the nominal strength in LWAC and PFLWAC-1 decreased by 17.1% and 12%, respectively. However, when the beam size increased from medium to large, the nominal strength in LWAC and PFLWAC-1 decreased by 20.6% and 20.4%, respectively. These results show that the role of polypropylene fibers in reducing the size dependency of strength gradually became negligible and insignificant for larger structures. Therefore, the utilization of polypropylene fibers for the purpose of reducing the size dependency of strength in small structures was more significant than large ones for LWAC. Analyzing the experimental results by the Design-Expert [25], the following relationship has been suggested for the σ_N that depends on the V_{pf}(%) and the d (mm):

$$\sigma_N = 0.92 + 0.36V_{pf} - 0.00256d + 0.00003V_{pf}.d - 0.26{V_{pf}}^2 + 0.000004d^2 (R^2 = 0.97). \quad (13)$$

4.4 Size effect on the material ductility

The other effect of specimen size is on the ductility of materials. Bažant demonstrated this effect by demonstrating the stress-relative deflection for each mixture based on the energy criterion [20]. The load-midspan deflection curves are provided in Fig. 12, while the stress-relative deflection curves are exhibited in Fig. 13. It was clear in Fig. 12 that when the size of specimens increased from small to large, the load resistance was enhanced. However, when the size of notched beams increased from small to large, each mixture demonstrated less relative deflection and the post-peak response descended steeper, according to Fig. 13. Based on the energy criterion, the main reason for this mechanism is the amount of strain energy to drive the propagation of the failure zone in each specimen [20]. The amount of strain energy enhances as the size of specimens increases. The increase of this energy enhances the brittleness and

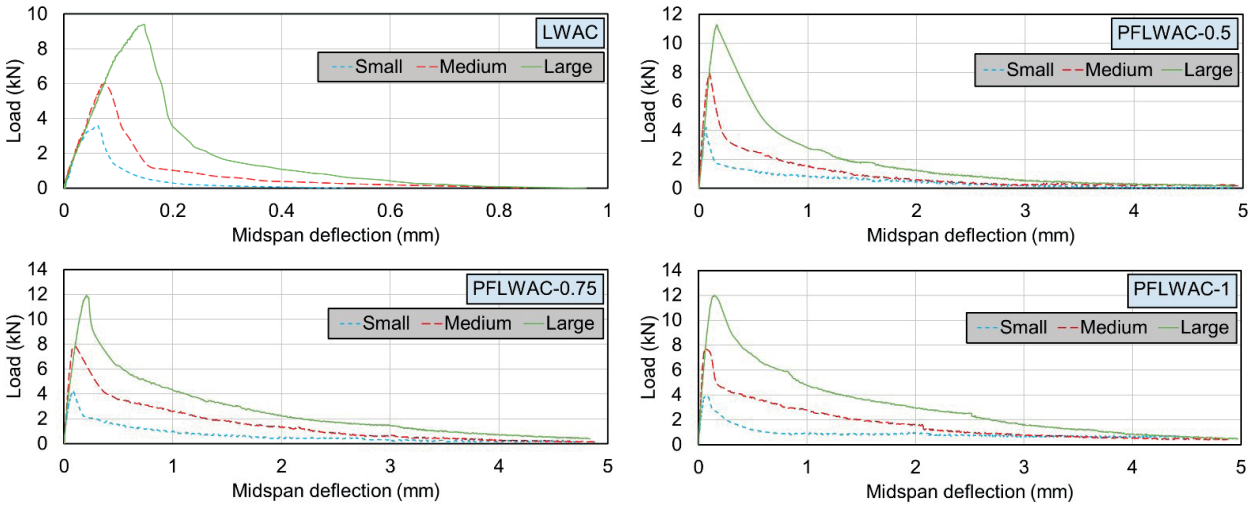

Fig. 12 Load-midspan deflection curves for each mix design

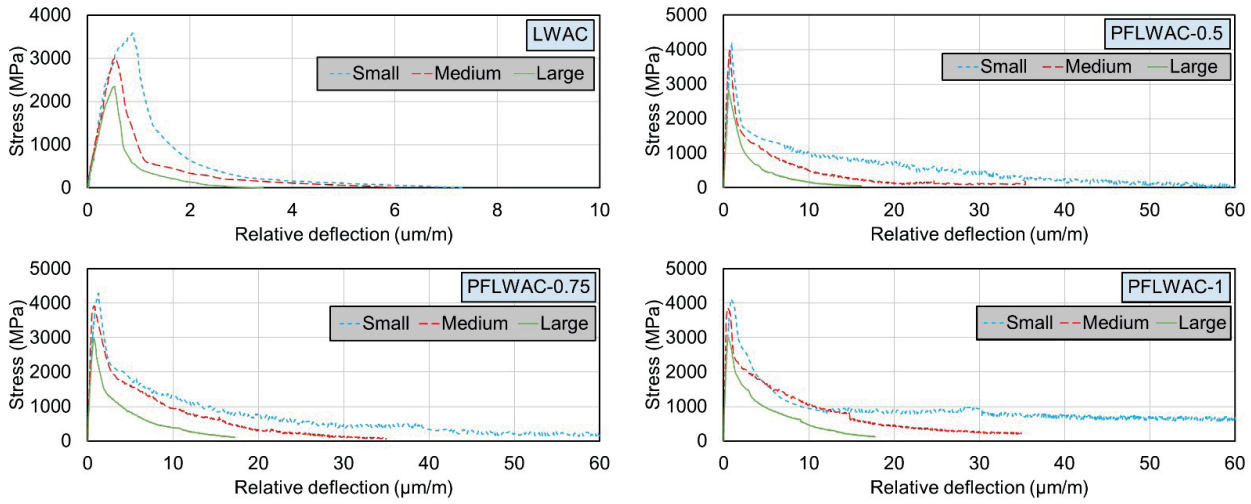

Fig. 13 Stress-relative deflection curves for each mix design

decreases the ductility of each specimen. Thus, the larger specimens in each mixture released greater amounts of strain energy to overcome the fracture process zone and exhibited lower ductility than smaller ones.

Fig. 14 demonstrates the stress-relative deflection curves up to the relative deflection of 3 (μm/m). It was noticeable in Fig. 14 that the post-peak behavior of larger specimens gradually approached smaller ones and descended slowly as the polypropylene fibers increased in LWAC. This result may be attributed to the amounts of polypropylene fibers stored in the initial ligament area of each size of notched beams. According to Fig. 15, small amounts of polypropylene fibers can be seen in the small-sized notched beam. As the size of notched beams increased from small to large in PFLWAC-1, the amounts of polypropylene fibers enhanced at the cross-section of notched beams. As illustrated in Fig. 15, large amounts of polypropylene fibers were concentrated at the cross-section of large specimens compared to small ones. This increase in the amounts of polypropylene fibers improved the post-peak response, the tensile ductility, and the length of fracture process zone at the tip of notch and reduced the amount of released strain energy to propagate the failure zone in larger specimens. The decrease of strain energy resulted in the reduction of size effect on the ductility of large specimens and approached their post-peak behavior to small ones. Moreover, the post-peak behavior descended slowly in large notched beams when the dosage of polypropylene fibers increased in LWAC. Therefore, the polypropylene fibers effectively decreased the size effect on the post-peak response and the ductility of specimens in LWAC. The fracture path of each geometrically similar notched beam in these four mixtures is illustrated in Fig. 16.

According to Fig. 16, the fracture path became more tortuous as the size of notched beams decreased from large to small. In other words, the fracture path was straight in large specimens, whereas it was tortuous in small ones. This tortuosity may be due to the bridging and aggregate interlocking in the fracture surface of concrete, which increases the energy absorption and the length of fracture process zone [46]. In fact, when the fracture path is more tortuous, the work required to have the crack propagation

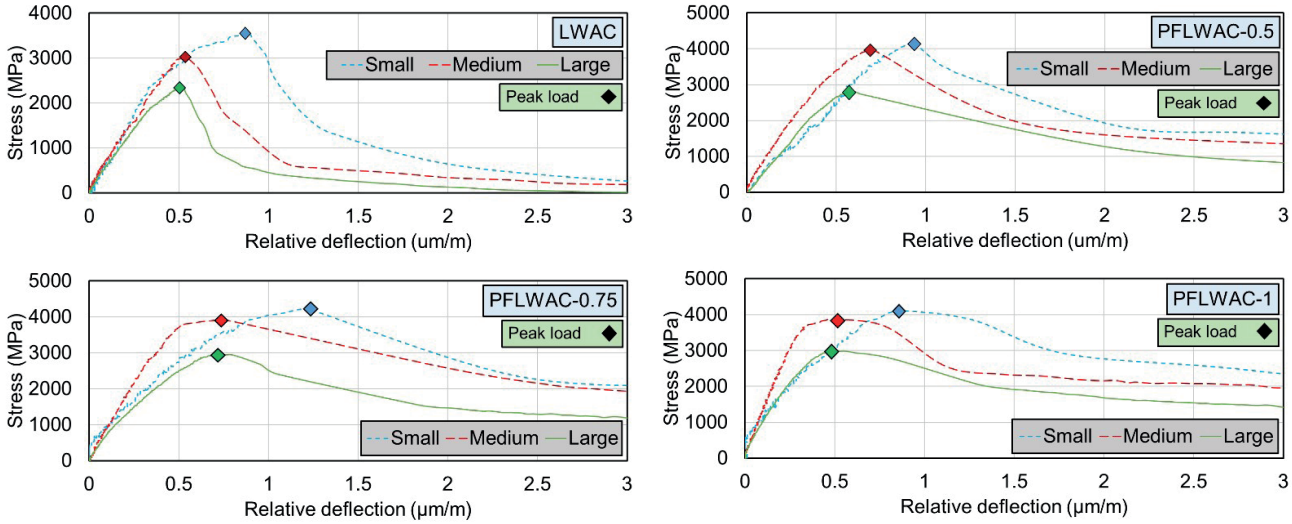

Fig. 14 Stress-relative deflection curves up to the relative deflection of 3 (μm/m)

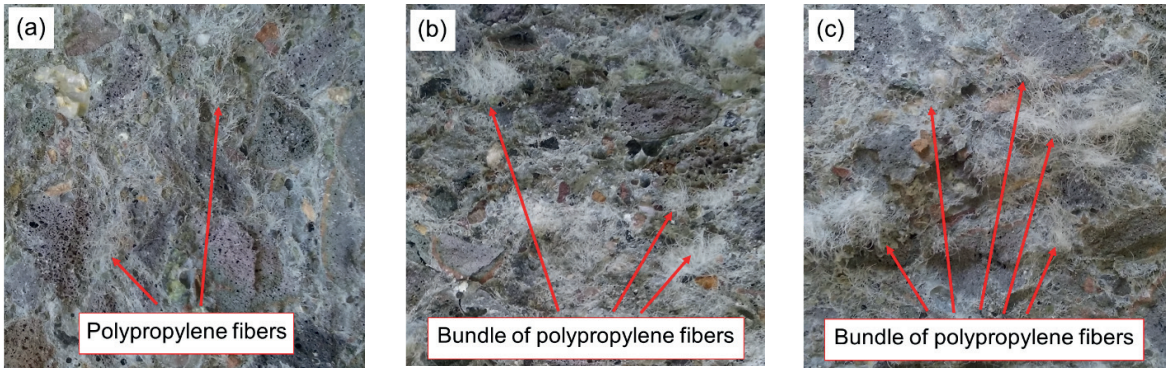

Fig. 15 The amounts of polypropylene fibers in various size of notched beams in the PFLWAC-1 mixture: (a) small, (b) medium, and (c) large

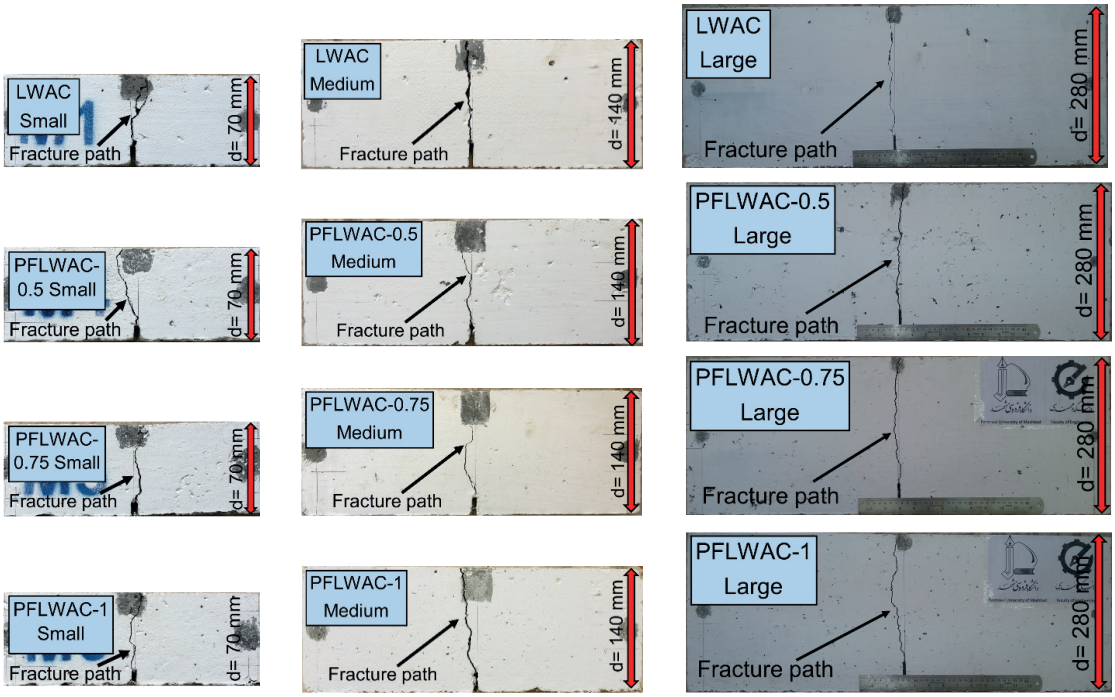

Fig. 16 Fracture path of geometrically similar notched beams of each mixture

should cross longer path, and higher amounts of energy are dissipated. In other words, the length of fracture process zone and the ductility are significant as the crack path is tortuous. Thus, high amounts of energy were absorbed in small notched beams compared to large ones. On the other hand, the incorporation of polypropylene fibers increased the tortuosity of fracture path in LWAC. As shown in Fig. 16, for medium-sized notched beams, the straight fracture path in LWAC turned into the tortuous fracture path as the 0.5%, 0.75%, and 1% volume contents of polypropylene fibers were employed in LWAC. Besides, the fracture path of large notched beams in PFLWAC-1 was more tortuous than the other mixtures. These results may be due to the characteristics such as the bridging mechanism and prohibiting the growth and propagation of cracks of polypropylene fibers, which resulted in the tortuosity of the fracture path and increased the energy dissipation and the length of fracture process zone for LWAC.

4.5 Size effect on the material fracture properties

In contrast to the initial fracture energy (G_f) derived from SEM, the total fracture energy (G_F) obtained from WFM is size-dependent. This size dependency has restricted the role of G_F as a material property [34, 47]. The size dependency of G_F in WFM has been used as a criterion for investigating the size dependency of fracture properties in most studies [4]. In fact, the amounts of G_F for various plain concretes increased as the size of structures increased [4, 35]. This increase in the amount of G_F for plain conventional concrete was more than 50% [37], while it was higher than 100% for plain LWAC due to the low tensile strength and specific weight of LWAC [4]. To investigate the size dependency of G_F in LWAC and PFLWACs, the G_F for geometrically similar notched beams of 190 × 70 × 70, 380 × 70 × 140, and 760 × 70 × 280 mm (length × width × depth) was calculated. The results of G_F for each beam size are shown in Table 7.

According to Table 7, the G_F in LWAC increased by 53.3% as the beam size increased from small to large. It can be seen that the G_F in LWAC increased less than that in the study conducted by Sim et al. [4]. However, this increase indicates that the G_F depended on the size of specimens in plain LWAC. The incorporation of 0.5%, 0.75%, and 1% volume content of polypropylene fibers in LWAC reduced the increase in the value of G_F as the beam size increased from small to large. The G_F reached almost the same values for different size notched beams at 1% volume fraction of polypropylene fibers. Incorporating polypropylene fibers increases the ductility and uniformly distributes the absorbed energy all around the bulk of LWAC specimens [45]. Thus, the polypropylene fibers could effectively decrease the dependency of G_F on the size effect parameter, and the G_F obtained from WFM for PFLWAC could be considered as a material property. Moreover, since the WFM considered the post-peak behavior of PFLWACs and the size dependency of its fracture parameters decreased due

Table 7 The fracture parameters of geometrically similar notched beams

Mixtures	Size	d (mm)	w_{t1} (N.m)	w_{t2} (N.m)	w_{t3} (N.m)	$w_{t\,ave}$ (N.m)	C.V. (%)	G_F (N/m)	l_{ch} (mm)
LWAC	Small	70	0.41	0.4	0.34	0.38	0.25	96.9	370.4
	Medium	140	0.99	0.92	0.98	0.96	0.1	122.4	467.9
	Large	280	2.26	2.37	2.36	2.33	0.1	148.6	568
PFLWAC-0.5	Small	70	2.68	2.64	2.73	2.68	0.05	683.7	1604.6
	Medium	140	5.38	5.55	5.42	5.45	0.1	695.2	1631.6
	Large	280	13.16	13.39	12.91	13.15	0.29	838.6	1968.1
PFLWAC-0.75	Small	70	2.99	3.17	3.34	3.17	0.64	808.7	1351.5
	Medium	140	8.28	7.79	7.87	7.98	0.58	1017.9	1701.2
	Large	280	15.81	15.82	15.86	15.83	0.01	1009.6	1687.3
PFLWAC-1	Small	70	4.47	4.39	4.56	4.47	0.11	1140.3	2440.6
	Medium	140	9.18	8.93	8.54	8.88	0.78	1132.7	2424.3
	Large	280	18.02	18.28	18.58	18.29	0.28	1166.5	2496.7

to the addition of polypropylene fibers, it can be concluded that WFM was suitable in order to investigate the fracture properties of LWAC containing high volume contents of polypropylene fibers. The relationship for G_F based on two main parameters such as V_{pf}(%) and d (mm) is obtained as:

$$G_F = -14.05 + 1402.34V_{pf} + 1.33d + 0.043V_{pf}.d - 387.37{V_{pf}}^2 - 0.0024d^2 \left(R^2 = 0.989\right). \quad (14)$$

4.6 The relationship between WFM and SEM

According to the bilinear softening curve of concrete in the cohesive crack model, the G_F derived from WFM corresponds to the total area under the entire bilinear softening curve, and the G_F derived from SEM corresponds to the area under the initial slope of the bilinear softening curve [48]. In many studies, the relation between these two methods was introduced by considering the ratio of G_F/G_f [16, 17, 22, 49]. Bažant and Becq-Giraudon [49] pointed out that the G_F/G_f ratio was 2.5 for normal concrete with a variation coefficient of 40%. Kazemi et al. [17] reported that the G_F/G_f ratio was 2.5 for high-strength concrete and 10.6 for steel fiber reinforced high-strength concrete. Ghasemi et al. [22] determined this ratio for the steel fiber reinforced self-compacting concrete to be equal to 9.66 with a coefficient of variation of 32%. In the current study, the G_F/G_f values for each mixture are listed in Table 8.

Table 8 Relationship between G_F/G_f ratio

Mixtures	V_{pf} (%)	G_F	G_f	G_F/G_f
LWAC	0	106.3	36.9	2.88
PFLWAC-0.5	0.5	513.5	52.9	9.71
PFLWAC-0.75	0.75	881.7	62.6	14.08
PFLWAC-1	1	730.7	56.2	13

The average value of G_F/G_f ratio for the PFLWACs was 12.26, with a variation coefficient of 28.17%.

5 Conclusions

This experimental research was conducted on geometrically similar notched beams with different dimensions of 190 × 70 × 70 mm^3 (small), 380 × 70 × 140 mm^3 (medium), and 760 × 70 × 280 mm^3 (large) employing size effect method (SEM) and notched beams with dimension of 350 × 100 × 100 mm3 using work of fracture method (WFM) to investigate the size effect and fracture properties of lightweight aggregate concrete (LWAC) under different volume fractions of polypropylene fibers. Accordingly, the following results were obtained:

- Results show that the fracture parameters obtained from SEM and WFM generally depended on the volume content of polypropylene fibers. The total fracture energy (G_F), the initial fracture energy (G_f), and the critical stress intensity factor (K_{IC}) of LWAC improved significantly when the polypropylene fibers increased.
- The nominal strength (σ_N) obtained from Bažant's size effect law for all the mix designs decreased with the increase in the size of notched beams. This decrease exhibits the size effect on the strength of LWAC. The increase in the volumetric content of polypropylene fibers in LWAC slightly reduced the decrease of strength due to the increase in the beam size. In other words, the polypropylene fibers relatively reduced the dependence of strength on the size effect parameter. Besides, the role of polypropylene fibers in reducing size dependency of strength for LWAC became negligible in large structures.

- According to the load-deflection curves of notched beams, the post-peak response of each mixture descended steeper and sustained less deflection as the size of notched beams increased. Furthermore, the tortuosity of crack path decreased when the beam size increased. These results demonstrated the size dependency of ductility and post-peak softening response in LWAC. However, the incorporation of polypropylene fibers in LWAC gradually approached the post-peak behavior in large notched beams ($760 \times 70 \times 280$ mm^3) to small ones ($190 \times 70 \times 70$ mm^3) and increased the tortuosity of fracture path. In conclusion, the incorporation of polypropylene fibers effectively enhanced the size independency of ductility.
- The total fracture energy in plain LWAC increased by 53.3% as the notched beam size increased. This increase in the amounts of fracture energy demonstrates the size dependency of fracture energy. The incorporation of polypropylene fibers in LWAC decreased the increase of total fracture energy due to the increase in the size of beam. Therefore, the polypropylene fibers significantly decreased the size dependency of fracture energy in LWAC.
- The main effect of polypropylene fibers was on the post-peak region of the load-midspan deflection curve of LWAC. Since the WFM considered the post-peak softening curve, the total fracture energy derived from this method was more significant than the initial fracture energy obtained from SEM in order to investigate the behavior of LWAC containing high volume fractions of polypropylene fibers. Moreover, the size dependency of fracture energy in this method decreased as the polypropylene fibers were used in LWAC.
- Since the SEM only considered the maximum applied load of specimens to determine the fracture parameters and its parameters were not size-dependent, the accuracy of this method was appropriate and acceptable for plain LWAC. However, the fracture parameters obtained from WFM exhibited significant size effect in plain LWAC. Thus, the WFM was not appropriate for determining the fracture properties of plain LWAC.
- The brittleness (β) decreased, and the characteristic length (l_{ch}) and the length of fracture process zone (c_f) increased when the volume fraction of polypropylene increased. A lower β and a larger l_{ch} and c_f indicated more ductile behavior in LWAC owing to the addition of polypropylene fibers.
- The total-to-initial fracture energy ratio (G_F/G_f) for plain LWAC was 2.88. In addition, the average value of G_F/G_f ratio in polypropylene fiber reinforced lightweight aggregate concrete mixes was 12.26, with a variation coefficient of 28.17%.

Nomenclature

Acronyms

LWAC	lightweight aggregate concrete
PFLWAC	polypropylene fiber reinforced lightweight aggregate concrete
SEM	size effect method
WFM	work of fracture method
NLFM	nonlinear fracture mechanics
LEFM	linear elastic fracture mechanics

Symbols

G_F	total fracture energy
G_f	initial fracture energy
l_{ch}	characteristic length
c_f	length of fracture process zone
K_{IC}	critical stress intensity factor
w_0	area under load-displacement curve
α	initial notch to depth ratio
ω_A	variation coefficient of slope
ω_C	variation coefficient of intercept
M	relative width of scattering bond
V_{pf}	polypropylene fiber volume fraction
P_0	corrected maximum load
A	slope of regression line
C	y-intercept of regression line
σ_N	nominal strength
a_0	initial notch length
b	width of beam
d	depth of beam
S	span of beam
L	length of beam
$g(\alpha_0)$	dimensionless geometric factor
E	modulus of elasticity
f_t	splitting tensile strength
f_c	compressive strength
δ_0	displacement at zero loading

References

[1] Li, J., Niu, J., Wan, C., Liu, X., Jin, Z. "Comparison of Flexural Property between High Performance Polypropylene Fiber Reinforced Lightweight Aggregate Concrete and Steel Fiber Reinforced Lightweight Aggregate Concrete", Construction and Building Materials, 157, pp. 729–736, 2017. https://doi.org/10.1016/j.conbuildmat.2017.09.149

[2] Wei, H., Wu, T., Yang, X. "Properties of Lightweight Aggregate Concrete Reinforced with Carbon and/or Polypropylene Fibers", Materials, 13(3), 640, 2020. https://doi.org/10.3390/ma13030640

[3] Güneyisi, E., Gesoglu, M., Özturan, T., Ipek, S. "Fracture Behavior and Mechanical Properties of Concrete with Artificial Lightweight Aggregate and Steel Fiber", Construction and Building Materials, 84, pp. 156–168, 2015. https://doi.org/10.1016/j.conbuildmat.2015.03.054

[4] Sim, J.-I., Yang, K.-H., Lee, E.-T., Yi, S.-T. "Effects of Aggregate and Specimen Sizes on Lightweight Concrete Fracture Energy", Journal of Materials in Civil Engineering, 26(5), pp. 845–854, 2014. https://doi.org/10.1061/(ASCE)MT.1943-5533.0000884

[5] Badogiannis, E. G., Christidis, K. I., Tzanetatos, G. E. "Evaluation of the Mechanical Behavior of Pumice Lightweight Concrete Reinforced with Steel and Polypropylene Fibers", Construction and Building Materials, 196, pp. 443–456, 2019. https://doi.org/10.1016/j.conbuildmat.2018.11.109

[6] Libre, N. A., Shekarchi, M., Mahoutian, M., Soroushian, P. "Mechanical Properties of Hybrid Fiber Reinforced Lightweight Aggregate Concrete Made with Natural Pumice", Construction and Building Materials, 25, pp. 2458–2464, 2011. https://doi.org/10.1016/j.conbuildmat.2010.11.058

[7] Sahoo, S., Selvaraju, A. K., Prakash, S. S. "Mechanical Characterization of Structural Lightweight Aggregate Concrete Made with Sintered Fly Ash Aggregates and Synthetic Fibres", Cement and Concrete Composites, 103712, 2020. https://doi.org/10.1016/j.cemconcomp.2020.103712

[8] Sahoo, S., Lakavath, C., Prakash, S. S. "Experimental and Analytical Studies on Fracture Behavior of Fiber-Reinforced Structural Lightweight Aggregate Concrete", Journal of Materials in Civil Engineering, 33(5), 2021. https://doi.org/10.1061/(ASCE)MT.1943-5533.0003680

[9] Zohrabi, M., Zohrabi, A., Chermahini, A.G. "Investigation of the Mechanical Properties of Lightweight Concrete Containing LECA with Metakaoline Pozzolan Using Polypropylene and Steel Fibers", Journal of Applied Environmental and Biological Sciences, 5(12S), pp. 11–15, 2015.

[10] Li, J., Niu, J., Wan, C., Jin, B., Yin, Y. "Investigation on Mechanical Properties and Microstructure of High Performance Polypropylene Fiber Reinforced Lightweight Aggregate Concrete", Construction and Building Materials, 118, pp. 27–35, 2016. https://doi.org/10.1016/j.conbuildmat.2016.04.116

[11] Li, J., Wan, C., Zhang, X., Niu, J. "Fracture Property of Polypropylene Fiber Reinforced Lightweight Concrete at High Temperatures", Magazine of Concrete Research, 72(22), pp. 1147–1154, 2020. https://doi.org/10.1680/jmacr.17.00432

[12] Alberti, M. G., Enfedaque, A., Gálvez, J. C., Cánovas, M. F., Osorio, I. R. "Polyolefin Fiber-Reinforced Concrete Enhanced with Steel-Hooked Fibers in Low Proportions", Materials and Design, 60, pp. 57–65, 2014. https://doi.org/10.1016/j.matdes.2014.03.050

[13] Shah, S. P., Swartz, S. E., Ouyang, C. "Fracture Mechanics of Concrete Applications of Fracture Mechanics to Concrete, Rock and Other Quasi-Brittle Materials", John Wiley and Sons, 1995. ISBN: 978-0-471-30311-4

[14] RILEM TC-50 FMC "Determination of the Fracture Energy of Mortar and Concrete by Means of Three-point Bend Tests on Notched Beams", Materials and Structures, 18, pp. 287–290, 1985. https://doi.org/10.1007/BF02472918

[15] RILEM TC-89 "Size-Effect Method for Determining Fracture Energy and Process Zone Size of Concrete", Materials and Structures, 23, pp. 461–465, 1990. https://doi.org/10.1007/BF02472030

[16] Mousavi, S. M., Ranjbar, M. M., Madandoust, R. "Combined Effects of Steel Fibers and Water to Cementitious Materials Ratio on the Fracture Behavior and Brittleness of High Strength Concrete", Engineering Fracture Mechanics, 216, 106517, 2019. https://doi.org/10.1016/j.engfracmech.2019.106517

[17] Kazemi, M. T., Golsorkhtabar, H., Beygi, M. H. A., Gholamitabar, M. "Fracture Properties of Steel Fiber Reinforced High Strength Concrete Using Work of Fracture and Size Effect Methods", Construction and Building Materials, 142, pp. 482–489, 2017. https://doi.org/10.1016/j.conbuildmat.2017.03.089

[18] Xie, C., Cao, M., Khan, M., Yin, H., Guan, J. "Review on Different Testing Methods and Factors Affecting Fracture Properties of Fiber Reinforced Cementitious Composites", Construction and Building Materials, 273, 121766, 2021. https://doi.org/10.1016/j.conbuildmat.2020.121766

[19] Rasheed, M. A., Prakash, S. S., Raju, G., Kawasaki, Y. "Fracture Studies on Synthetic Fiber Reinforced Cellular Concrete Using Acoustic Emission Technique", Construction and Building Materials, 169, pp. 100–112, 2018. https://doi.org/10.1016/j.conbuildmat.2018.02.157

[20] Bažant Z. P., Planas, J. "Fracture and Size Effect in Concrete and Other Quasi-Brittle Materials", CRC Press, 1998. ISBN 97808 49382840

[21] Dehestani, M., Nikbin, I. M., Asadollahi, S. "Effects of Specimen Shape and Size on the Compressive Strength of Self-Consolidating Concrete (SCC)", Construction and Building Materials, 66, pp. 685–691, 2014. https://doi.org/10.1016/j.conbuildmat.2014.06.008

[22] Ghasemi, M., Ghasemi, M. R., Mousavi, S. R. "Studying the Fracture Parameters and Size Effect of Steel Fiber-Reinforced Self-Compacting Concrete", Construction and Building Materials, 201, pp. 447–460, 2019. https://doi.org/10.1016/j.conbuildmat.2018.12.172

[23] Picazo, Á., Alberti, M. G., Gálvez, J. C., Enfedaque, A., Vega, A. C. "The Size Effect on Flexural Fracture of Polyolefin Fibre-Reinforced Concrete", Applied Sciences, 9 (9), 1762, 2019. https://doi.org/10.3390/app9091762

[24] Nguyen, D. L., Kim, D. J., Ryu, G. S., Koh, K. T. "Size Effect on Flexural Behavior of Ultra-High-Performance Hybrid Fiber-Reinforced Concrete", Composites: Part B, 45, pp. 1104–1116, 2013. https://doi.org/10.1016/j.compositesb.2012.07.012

[25] Stat-Ease, Inc. "Design-Expert (V13)", [Software] Available at: https://www.statease.com/software/design-expert

[26] Bažant, Z. P. "Size Effect in Blunt Fracture: Concrete, Rock, Metal", Journal of Engineering Mechanics, 110, pp. 518–535, 1984. https://doi.org/10.1061/(ASCE)0733-9399(1984)110:4(518)

[27] Bažant, Z. P. "Size Effect in Tensile and Compression Fracture of Concrete Structures: Computational Modeling and Design", Fracture Mechanics of Concrete Structures, 3, pp. 1905–1922, 1998.

[28] Bažant, Z. P. "Size Effect on Structural Strength: a Review", Archive of Applied Mechanics, 69, pp. 703–725, 1999. https://doi.org/10.1007/s004190050252

[29] Bažant, Z. P., Kazemi, M. T. "Determination of Fracture Energy, Process Zone Length and Brittleness Number from Size Effect, with Application to Rock and Concrete", International Journal of Fracture, 44, pp. 111–131, 1990. https://doi.org/10.1007/BF00047063

[30] Hillerborg, A., Modéer, M., Petersson, P.-E. "Analysis of Crack Formation and Crack Growth in Concrete by Means of Fracture Mechanics and Finite Element", Cement and Concrete Research, 6(6), pp. 773–782, 1976. https://doi.org/10.1016/0008-8846(76)90007-7

[31] Petersson, P.-E. "Crack Growth and Development of Fracture Zones in Plain Concrete and Similar Materials", Division of Building Materials, Lund Institute of Technology, Lund, Sweden, Rep. TVBM-1006, 1981.

[32] Swartz, S. E., Yap, S. T. "The Influence of Dead Load on Fracture Energy Measurements Using the Rilem Method", Materials and Structures, 21, pp. 410–415, 1988. https://doi.org/10.1007/BF02472320

[33] Hillerborg, A. "The Theoretical Basis of a Method to Determine the Fracture Energy GF of Concrete", Materials and Structures, 18(4), pp. 291–296, 1985. https://doi.org/10.1007/BF02472919

[34] Cifuentes, H., Alcalde, M., Medina, F. "Comparison of the Size-Independent Fracture Energy of Concrete Obtained by Two Test Methods", Strain, 49(1), pp. 54–59, 2013. https://doi.org/10.1111/str.12012

[35] Hillerborg, A. "Results of Three Comparative Test Series for Determining the Fracture Energy of Concrete", Materials and Structures, 18, pp. 407–413, 1985. https://doi.org/10.1007/BF02472416

[36] Elices, M., Guinea, G. V., Planas, J. "Measurement of the Fracture Energy Using Three-Point Bend Tests: Part 3 - Influence of Cutting the P-δ tail", Materials and Structures, 25, pp. 327–334, 1992. https://doi.org/10.1007/BF02472591

[37] Guinea, G. V., Planas, J., Elices, M. "Measurement of the Fracture Energy Using Three-Point Bend Tests: Part 1- Influence of Experimental Procedures", Materials and Structures, 25, pp. 212–218, 1992. https://doi.org/10.1007/BF02473065

[38] Planas, J., Elices, M., Guinea, G. V. "Measurement of the Fracture Energy Using Three-Point Bend Tests: Part 2- Influence of Bulk Energy Dissipation", Materials and Structures, 25, pp. 305–312, 1992. https://doi.org/10.1007/BF02472671

[39] Chinese Standard "GB/T17431.2 Lightweight Aggregates and Its Test Methods-Part 2: Test Methods for Lightweight Aggregates", Quality Supervision Inspection and Quarantine of the People's Republic of China and Standardization Administration of People's Republic of China, Beijing, China, 2010.

[40] ASTM "C143/C143M-05 Standard Test Method for Slump of Hydraulic Cement Concrete", American Society of Testing and Materials, West Conshohocken, PA, USA, 2005. https://doi.org/10.1520/C0143_C0143M-05

[41] Saradar, A., Tahmouresi, B., Mohseni, E., Shadmani, A. "Restrained Shrinkage Cracking of Fiber-Reinforced High-Strength Concrete", Fibers, 6(1), 12, 2018. https://doi.org/10.3390/fib6010012

[42] BS "BS EN 12390 Testing Hardened Concrete. Method of determination of Compressive Strength of Concrete Cubes, (BS, Part 3)", British Standards Institution, London, UK, 2000.

[43] ASTM "C496/C496M-11 "Standard Test Method for Splitting Tensile Strength of Cylindrical Concrete Specimens", American Society of Testing and Materials, West Conshohocken, PA, USA, 2011. https://doi.org/10.1520/C0496_C0496M-11

[44] ASTM "C469/C469M-04 "Standard Test Method for Static Modulus of Elasticity and Poisson's Ratio of Concrete in Compression", American Society of Testing and Materials, West Conshohocken, PA, USA, 2004. https://doi.org/10.1520/C0496_C0496M-04

[45] de Freitas, I., Darwish, F., Pereira, M. V., Allende, K. "Fracture Behavior of Polymeric Fiber Reinforced Lightweight Structural Concrete", Materials Research, 17(6), pp. 1588–1593, 2014. https://doi.org/10.1590/1516-1439.287314

[46] Sadrmomtazi, A., Lotfi-Omran, O., Nikbin, I. M. "Influence of Cement Content and Maximum Aggregate Size on the Fracture Parameters of Magnetite Concrete Using WFM, SEM and BEM", Theoretical and Applied Fracture Mechanics 107, 102482, 2020. https://doi.org/10.1016/j.tafmec.2020.102482

[47] Bencardino, F., Rizzuti, L., Spadea, G., Swamy, R. N. "Experimental Evaluation of Fiber Reinforced Concrete Fracture Properties", Composites: Part B, 41, pp. 17–24, 2010. https://doi.org/10.1016/j.compositesb.2009.09.002

[48] fib "CEB-FIP Mode Code 1990 - 1st Predraft - Vol. 1", Bulletin 190, International Federation for Structural Concrete, Lausanne, Switzerland, 1990.

[49] Bažant, Z. P., Becq-Giraudon, E. "Statistical Prediction of Fracture Parameters of Concrete and Implications for Choice of Testing Standard", Cement and Concrete Research, 32, pp. 529–556, 2002. https://doi.org/10.1016/S0008-8846(01)00723-2